

## Synthesis and application of colloidal CdS quantum dots as interface modification material in perovskite solar cells

Esma YENEL\* 

Department of Electricity and Energy, Konya Technical University, School of Technical Science, Konya Turkey

Received: 01.07.2021 • Accepted/Published Online: 16.09.2021 • Final Version: 20.12.2021

**Abstract:** In this study, colloidal CdS quantum dots were synthesized, structurally characterized, and their effect on performance of perovskite solar cells was observed by using them as interface modification agent between TiO<sub>2</sub>/perovskite. Colloidal CdS quantum dots were synthesized based on two-phase method and characterized by X-ray diffraction and Transmission Electron Microscopy techniques. The average particle size of CdS quantum dots have found to be around 5 nm. Oleic acid was used as capping agent during synthesis to lead solubility in organic solvents. Obtained quantum dots are coated on compact TiO<sub>2</sub> layer for surface modification. A decrease was observed when oleic acid capped CdS quantum dots were used at interface, while significant improvement was observed when ligand exchange was carried out by pyridine before perovskite layer. Reference solar cells showed 11.6% efficiency, while pyridine capped CdS modified solar cells' efficiency was 13.2%. Besides the improvement in efficiency, reproducibility of solar cells also was increased by using pyridine capped CdS as interface material.

**Key words:** Colloidal CdS quantum dots, perovskite solar cells

### 1. Introduction

Recently, due to their low cost, high efficiency, and facile fabrication, perovskite solar cells have become more attractive for many researchers. Since Miyasaka and co-workers firstly reported in 2009, perovskite solar cell (PSC) technology has undergone an improvement from 3.8% to around 25% [1,2]. A basic perovskite solar cell consists of a transparent conductive layer such as Fluorine doped Tin Oxide (FTO) or Indium doped Tin Oxide (ITO), an electron transport layer, light sensitive perovskite layer, a hole transport layer, and finally a metal electrode. As it is valid for all layers, electron transport layer plays an important role for high efficiency in PSCs. TiO<sub>2</sub> is one of the most used electron transport layer due to its' various fabrication method such as spin coating, spray coating, sputter, etc. [3–5]. Independent from preparation technique, TiO<sub>2</sub> structure includes some problems such as oxygen vacancies and nonstoichiometric defects especially located on TiO<sub>2</sub> surface [6,7]. Those defects prevent electron flow that results in bad performance of perovskite solar cells. Some of researchers reported some different materials such as SnO<sub>2</sub>, ZnO, CdS and WO<sub>x</sub> instead of TiO<sub>2</sub> as electron transport layer [8–11]. Although CdS as an electron transport layer is still far from satisfactory, it may be an excellent interface material for modification and passivation of TiO<sub>2</sub> surface. Recently, Hwang et al. reported that CdS, as a modification material for mesoporous TiO<sub>2</sub> layer, lead improvement in stability of perovskite solar cells [12]. Zhao et al. used CdS as an additive to precursor solution and observed significant reduction in recombination [13]. Dong et al. used CdS as electron transport layer and observed 16.5% efficiency in PSCs [14]. Wessendorf et al. observed a decrease in hysteresis by using CdS as electron transport layer [15]. Cd diffusion through to perovskite layer leads an increase in grain size resulting better efficiency [16]. Mohamadkhania et al. used CdS on SnO<sub>2</sub> surface as interface modifier and observed decrease in hysteresis and increase in efficiency [17]. Ma et al. showed that chemically deposited CdS on TiO<sub>2</sub> surface improves the efficiency from 10.31% to 14.26% [18].

In this work, different from the other works previously reported, we used colloidal CdS quantum dots for modification of TiO<sub>2</sub> surface. Firstly, we synthesized oleic acid capped CdS and directly used those materials as interface agent. For comparison, we carried out ligand exchange procedure with pyridine to obtain pyridine capped CdS. Pyridine is a small and electron-rich molecules that it contributes electron transfer in such devices. Some researchers used pyridine and similar small molecules between electron transport layer and perovskite layer [19]. In addition, pyridine can be easily

\* Correspondence: [esmayenel@gmail.com](mailto:esmayenel@gmail.com)

replaced with oleic acid without further chemical process. So, pyridine would be one of the best choices to eliminate oleic acids. Both types of CdS quantum dots were used at  $\text{TiO}_2$ /perovskite interface, and the results were compared with nonmodified PSCs.

## 2. Materials and methods

### 2.1. Synthesis of colloidal CdS quantum dots

In the synthesis of quantum dots, the two-phase method has been used. Quantum dots are obtained at the interface between the organic phase and the water phase. First, the sulphur source thiourea, which is used as a slow and controlled release agent by hydrolysis on the surface of cadmium myristate particles not fully dissolved in the water phase, is preferred. In the reaction medium to be created in this way, depending on the time and concentration, the particle grows very slowly and in a controlled manner at the interface. The applied synthesis method is given below.

Cadmium myristate particles start crystal formation on the surface, and then the growth of crystals was achieved at the interface. In the reaction added sulphur source thiourea, by controlled hydrolysis, provides sulphur to the environment. CdS cores will be created. The resulting structure is transferred from the interface to the organic phase with the help of the surfactant in toluene after the addition of the toluene phase. During this transition, growth will continue at the interface.

Separating the reacted parts of cadmium myristate from the surface of particles, the remaining cadmium myristate reacts rapidly with sulphur to form the same system. Particle formation will continue over it. 0.4 g cadmium myristate is suspended in 80 mL of water under argon at 100 °C for 15 min. At this stage, the solution of 0.060 g thiourea in 5 mL of water should be added to the medium by syringe. Immediately after, 80 mL of toluene containing 1 mL of oleic acid is added and continued to stir at 100 °C. A total of 2 mL of sampling is done every 30 min from toluene phase, and growth control of crystal with the aid of UV and fluorescence is done. At the end of the reaction, the quantum dots are removed from the organic phase with the help of ethanol separated by precipitation and stored for analysis. Samples taken during the reaction are also precipitated with ethanol and stored. Coated with surfactant materials such as electron-poor oleic acid, TOPO electron flow is low in solar cells produced with quantum dots. In cells produced with quantum dots coated with surface-active materials such as thiophene and pyridine, which are rich in electrons, electron flow is high due to conjugated bonds. Therefore, during the studies, electron-rich surfactants such as pyridine materials have been used.

### 2.2. Fabrication of perovskite solar cells

#### 2.2.1. Preparation of reference perovskite solar cells

Perovskite solar cells (PSCs) were fabricated on FTO coated glass. Fluorine doped tin oxide (FTO) coated glass substrates were cut into 1.5 cm×1.5 cm square pieces. FTO glass was ultrasonically cleaned with hellmanex, de-ionized water, acetone, and isopropyl alcohol for 10 min and dried with nitrogen. Before coating, oxygen plasma treatment was carried out to remove organic impurities and to activate the surface. Compact  $\text{TiO}_2$  layer was coated by spray coating technique.  $\text{TiO}_2$  solution was prepared by dissolving 3 mL of titanium isopropoxide in absolute ethanol. Another solution with 2 mL of acetylacetone in 6 mL of absolute ethanol was prepared. Acetylacetone solution was added to stirring titanium isopropoxide dropwise. The mixture was kept overnight by stirring at room temperature. Before spray coating, stock solution was 1:1 diluted with absolute ethanol. FTO glasses were heated to 450 °C and coated by spray then kept for 3 min at the same temperature and cooled down to room temperature slowly.

Perovskite in DMSO:DMF solvent was prepared according to previously published procedure Zhang et al [20]. The perovskite precursors, consisting of 922 mg  $\text{PbI}_2$  and 349.8 mg MAI were dissolved in 900  $\mu\text{L}$  DMF and 100  $\mu\text{L}$  DMSO. Then, perovskite layer was deposited statically by spin-coating at 6000 rpm for 30 s. A total of 100  $\mu\text{L}$  of sec butyl alcohol as antisolvent was dropped at 7th s during spinning. At the second step, sec-butyl alcohol was added statically on perovskite coated layer and kept for 12 s and spin coated at 6000 rpm for 30 s. Final perovskite films were dried at 100 °C for 30 min.

Spiro-OMeTAD solution consisting of 65 mg of spiro-OMeTAD, 20  $\mu\text{L}$  of 4-tert-butyl pyridine, 70  $\mu\text{L}$  of Li-TFSI (170mg mL<sup>-1</sup> in acetonitrile), and 1mL of chlorobenzene was prepared and spin-coated at 4000 rpm for 30 s onto perovskite layer.

Finally, 100 nm of Au was thermally evaporated onto HTM layer by using a shadow mask. Active area of each electrode was calculated to be 0.023 cm<sup>2</sup>.

#### 2.2.2. Preparation of oleic acid and pyridine capped perovskite solar cells

For OA-CdS modified perovskite solar cells, oleic acid capped quantum dots dissolved in chlorobenzene (5 mg/mL) were spin casted onto  $\text{TiO}_2$  surface at 5000 rpm for 40s and dried at 100 °C for 5 min. Then, perovskite solution was spin casted as explained in text above. PYR-CdS modified solar cells were prepared by pyridine washing after coating OA capped CdS. For this concept, after coating OA capped CdS on  $\text{TiO}_2$  surface, 70  $\mu\text{L}$  pyridine was dropped on film during spinning at 5000 rpm and then dried at 100 °C 5 min. After pyridine treatment, perovskite layer was deposited as explained above.

### 2.2.3. Characterizations of perovskite solar cells

IV characterizations were carried out in nitrogen filled glove box system under AM 1.5 solar simulator by Keithley 2400 power source. Light intensity was measured with a calibrated KIPP&ZONEN pyromometer and calculated to be 80 mW/cm<sup>2</sup>

### 3. Results and discussion

The XRD spectrum of CdS quantum dots showed that the crystal structure of CdS QDs is cubic with an excellent match to XRD spectrum of cubic bulk CdS (JCPDS no. 10-0454). XRD spectrum of CdS quantum dots had 3 peaks at 26.6° (corresponds to 111 plane of cubic CdS), 44.11° (corresponds to 200 plane of cubic CdS), and 52.26° (corresponds to 311 plane of cubic CdS). These 3 peaks are typical 2 $\theta$  values for cubic CdS crystal (JCPDS no. 10-0454). Also, the broadening in these peaks was a proof of quantum dot formation. By applying Scherrer equation, the size of CdS quantum dots were found to be 5 nm (see Figure 1). Transmission electron microscopy images also supports the formation of CdS quantum dots (see Figure 2). It is clear from the Figure 1 that average particle size of quantum dots is approximately 5 nm, and a homogenous particle size distribution is observed.

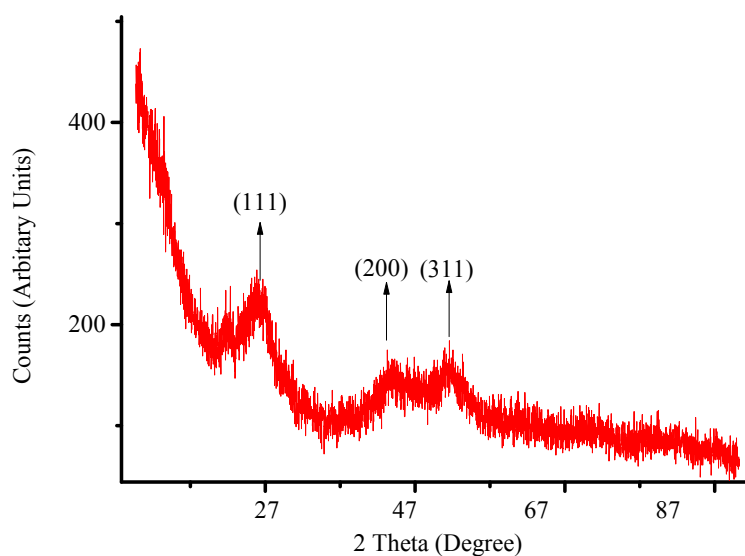


Figure 1. XRD spectra of colloidal CdS quantum dots.

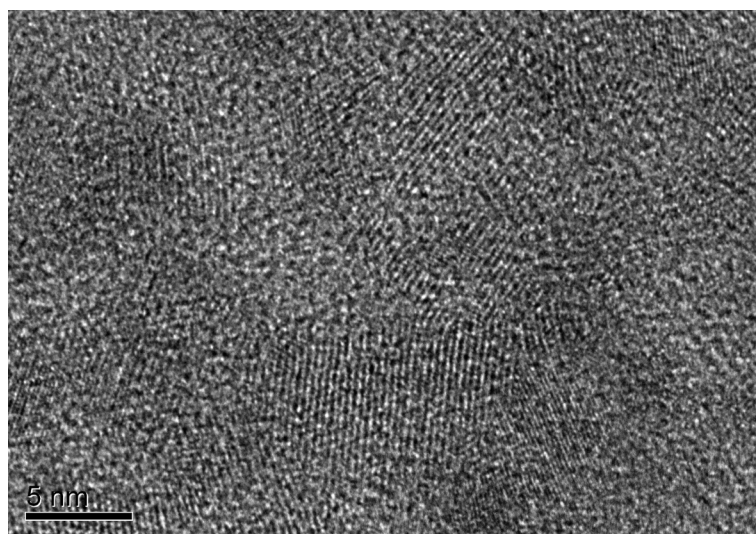


Figure 2. TEM pictures of CdS quantum dots.

Synthesized quantum dots are used as interface layer between  $\text{TiO}_2$  and perovskite layer in forms of oleic acid capped and pyridine capped. Figure 3 shows IV characterizations of reference and CdS included perovskite solar cell. As it is clear from Figure 3 and Table, oleic acid capped CdS lead a decrease from 11.7% to 10.5% in PSCs' performance. This is most probably due to long hydrocarbon chain of the capping agent the prevent electron injection in such devices. Oleic acid has 18 carbons, which means that it takes too long for hopping process of electrons from one side to other side. However, in case pyridine capped CdS, performance of PSCs is obviously increased from 11.7% to 13.2%. At first, this improvement may be attributed to UV absorption of CdS and its' contribution to electron transfer process. If this comment was true, we should have observed improvement for both OA and pyridine capped CdS. However, pyridine capped CdS show improvement, while it is vice versa for OA capped. The role of OA is discussed above. So, we may suggest that the absorption of CdS does not influence the electron transfer, therefore, efficiency. This improvement may be attributed to two reasons. The first one may be the basic explanation that electron rich structure and molecular volume of pyridine facilitate electron transfer from perovskite to  $\text{TiO}_2$ . Pyridine, due to its' molecular structure, passivates the surface states of CdS quantum dots; besides, it provides an electron rich media that facilitate electron hopping process. The second one can be attributed to the coordination of excess amount of pyridine to the uncoordinated  $\text{Pb}^{2+}$  ions that increases crystal quality of perovskite, which results in better performance of PSCs. As well known in literature, uncoordinated  $\text{Pb}^{2+}$  in perovskite layer immigrates through to HTM layer and this movement dramatically decrease stability and efficiency of PSCs [21,22]. Xue et al. reported that amino and hydroxy groups facilitate crystal formation of perovskite and coordinate to the uncoordinated  $\text{Pb}^{2+}$  [23]. Similar process may occur in case pyridine existence at  $\text{TiO}_2$ /perovskite interface.

Table summarized the performance parameters of PSCs. In all cases,  $V_{oc}$  values are observed to be 950 mV, while  $I_{sc}$  values varies from 18.14 to 20.6 depending on efficiency. As explained above, observation of low current in OA capped CdS is most probably due to long hydrocarbon chain of oleic acid side. On the other hand, better current values are observed in case pyridine capped CdS that support our attributions. Beside  $I_{sc}$  values, FF values are also improved by pyridine capped CdS included PSCs.

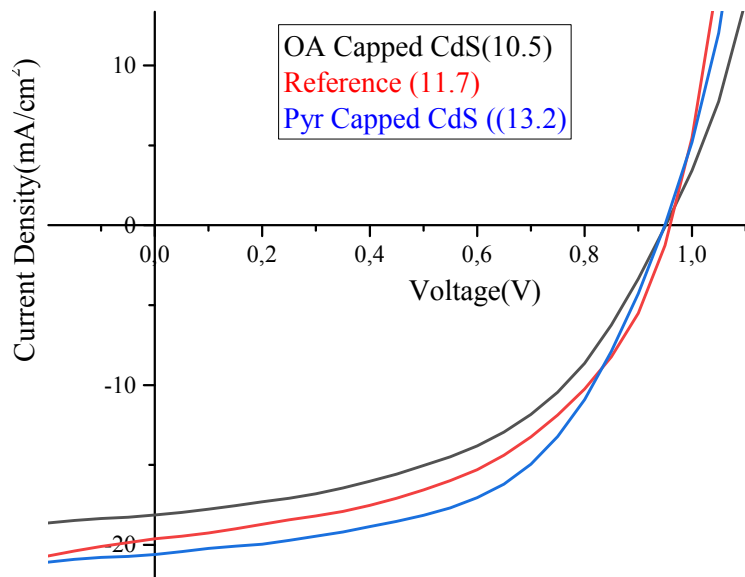
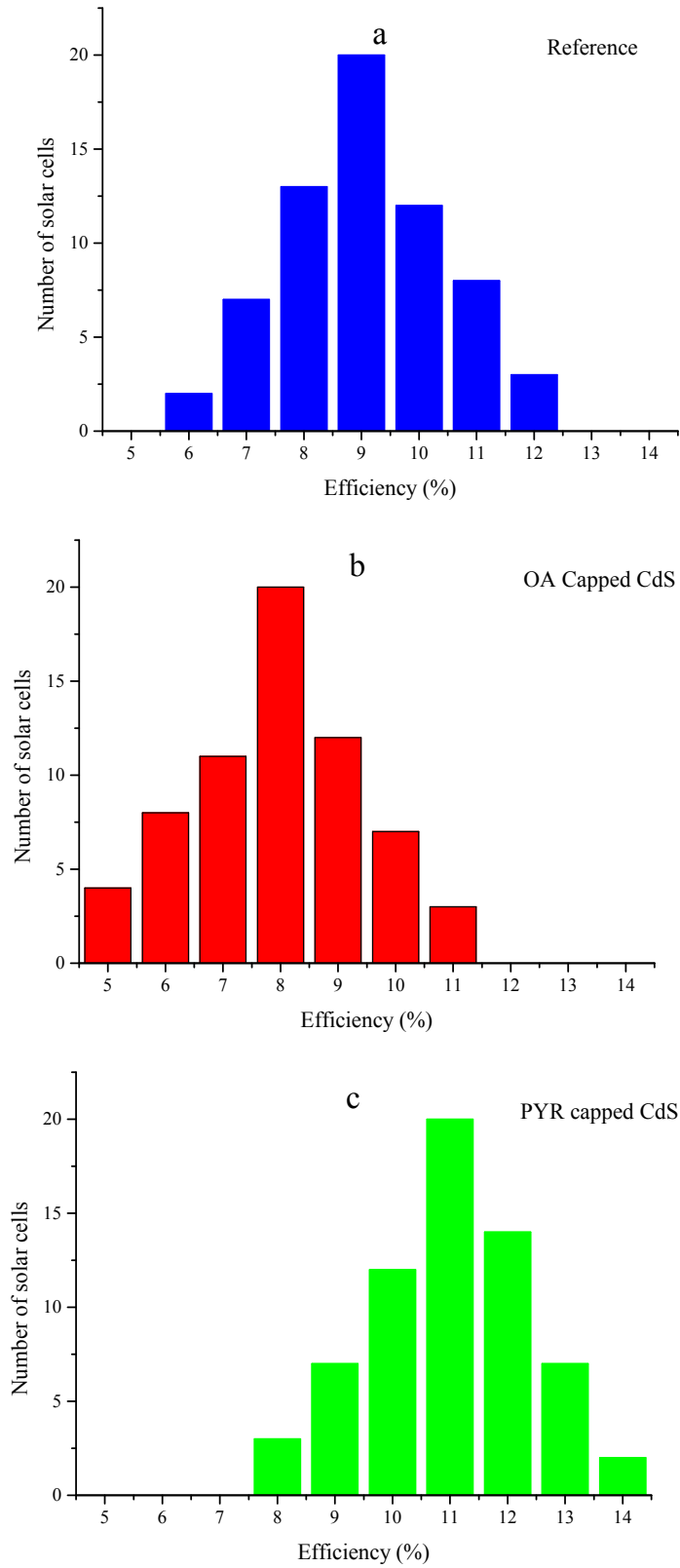


Figure 3. IV characterizations of perovskite solar cells.

Table. IV data of PSCs.

Concept	Efficiency	$I_{sc}$	$V_{oc}$	FF
Reference	11.7	19.65	950	0.50
CdS OA	10.5	18.14	950	0.49
CdS Pyr	13.2	20.6	950	0.54



**Figure 4.** Reproducibility results of PSCs. (a) refers to reference, (b) refers to oleic acid capped CdS layer included, and (c) refers to pyridine capped CdS included PSCs.

Reproducibility is another important parameter for PSCs. Reproducibility can be considered an indicator for crystal quality of perovskite. Figures 4a–4c show average efficiency values of a number of PSCs. It is clear from Figures 4a–4c that pyridine capped CdS significantly improves reproducibility of PSCs. Pyridine capped CdS included PSCs show narrower efficiency distribution than reference and OA capped CdS included PSCs. As discussed above, pyridine passivates CdS surface and fill electron traps as well as coordinates to uncoordinated  $\text{Pb}^{2+}$ , which increases crystal quality of perovskite layer.

#### 4. Conclusion

In this work, we focused on  $\text{TiO}_2$  and perovskite layer interface modification for better efficiency and reproducibility. The results showed that not only quantum dot type but also capping agent play an important role on efficiency and reproducibility of PSCs. Especially electron rich groups facilitate electron transfer from perovskite to  $\text{TiO}_2$  layer and increase crystal quality of perovskite by interaction with uncoordinated  $\text{Pb}^{2+}$  cations, which increases efficiency and reproducibility.

#### Acknowledgment

I would like to dedicate this work to my family and thank them for their lifelong support.

#### References

1. Kojima A, Teshima K, Shirai Y, Miyasaka T. Organometal halide perovskites as visible-light sensitizers for photovoltaic cells. *Journal of the American Chemical Society* 2009; 131 (17): 6050–6051.
2. Kim G, Min H, Lee KS, Lee DY, Yoon SM et al. Impact of strain relaxation on performance of a-formamidinium lead iodide perovskite solar cells. *Science* 2020; 370 (6512): 108–112. doi: 10.1126/science.abc4417
3. Heo JH, Lee MH, Han HJ, Patil BR, Yu JS et al. Highly efficient low temperature solution processable planar type  $\text{CH}_3\text{NH}_3\text{PbI}_3$  perovskite flexible solar cells. *Journal of Materials Chemistry A* 2016; 4 (5): 1572–1578. doi: 10.1039/c5ta09520d
4. Yang D, Yang R, Zhang J, Yang Z, Liu S et al. High efficiency flexible perovskite solar cells using superior low temperature  $\text{TiO}_2$ . *Energy and Environmental Science* 2015; 8 (11): 3208–3214. doi: 10.1039/c5ee02155c
5. Seo MS, Jeong I, Park JS, Lee J, Han IK et al. Vertically aligned nanostructured  $\text{TiO}_2$  photoelectrodes for high efficiency perovskite solar cells: Via a block copolymer template approach. *Nanoscale* 2016; 8 (22): 11472–11479. doi: 10.1039/c6nr01010e
6. Bi D, Yang L, Boschloo G, Hagfeldt A, Johansson EMJ et al. Effect of different hole transport materials on recombination in  $\text{CH}_3\text{NH}_3\text{PbI}_3$  perovskite-sensitized mesoscopic solar cells. *The Journal of Physical Chemistry Letters* 2013; 4: 1532–1536.
7. Hagfeldt A, Boschloo G, Sun L, Kloo L, Pettersson H. Dye-sensitized solar cells. *Chemical Reviews* 2010: 6595–6663.
8. Wang K, Shi Y, Li B, Zhao L, Wang W et al. Amorphous inorganic electron-selective layers for efficient perovskite solar cells: feasible strategy towards room-temperature fabrication. *Advanced Materials* 2016; 28 (9): 1891–1897. doi: 10.1002/adma.201505241
9. Chandiran AK, Abdi-Jalebi M, Yella A, Dar MI, Yi C et al. Quantum-confined  $\text{ZnO}$  nanoshell photoanodes for mesoscopic solar cells. *Nano Letters* 2014; 14 (3): 1190–1195. doi: 10.1021/nl4039955
10. Ke W, Fang G, Liu Q, Xiong L, Qin P et al. Lower temperature solution-processed tin oxide as an alternative electron transporting layer for efficient perovskite solar cells. *Journal of the American Chemical Society* 2015; 137 (21): 6730–6733. doi: 10.1021/jacs.5b01994
11. Liu J, Gao C, Luo L, Ye Q, He X et al. Low-temperature, solution processed metal sulfide as an electron transport layer for efficient planar perovskite solar cells. *Journal of Materials Chemistry A* 2015; 3 (22): 11750–11755. doi: 10.1039/c5ta01200g
12. Hwang I, Baek M, Yong K. Core/Shell structured  $\text{TiO}_2/\text{CdS}$  electrode to enhance the light stability of perovskite solar cells. *ACS Applied Materials and Interfaces* 2015; 7 (50): 27863–27870. doi: 10.1021/acsami.5b09442
13. Zhao W, Shi J, Tian C, Wu J, Li H, Li Y, et al. CdS induced passivation toward high efficiency and stable planar perovskite solar cells. *ACS Applied Materials & Interfaces* 2021; 13 (8): 9771–9780. doi: 10.1021/acsami.0c18311
14. Dong J, Wu J, Jia J, Fan L, Lin Y et al. Efficient perovskite solar cells employing a simply-processed CdS electron transport layer. *Journal of Materials Chemistry C* 2017; 5 (38): 10023–10028. doi: 10.1039/c7tc03343e
15. Wessendorf CD, Hanisch J, Müller D, Ahlswede E. CdS as electron transport layer for low-hysteresis perovskite solar cells. *Solar RRL* 2018; 2 (5): 1–10. doi: 10.1002/solr.201800056
16. Dunlap-Shohl WA, Younts R, Gautam B, Gundogdu K, Mitzi DB. Effects of Cd diffusion and doping in high-performance perovskite solar cells using CdS as electron transport layer. *Journal of Physical Chemistry C* 2016; 120 (30): 16437–16445. doi: 10.1021/acs.jpcc.6b05406

17. Mohamadkhani F, Javadpour S, Taghavinia N. Improvement of planar perovskite solar cells by using solution processed SnO<sub>2</sub>/CdS as electron transport layer. *Solar Energy* 2019; 191 (May): 647–653. doi: 10.1016/j.solener.2019.08.067
18. Ma Y, Deng K, Gu B, Cao F, Lu H et al. Boosting efficiency and stability of perovskite solar cells with CdS inserted at TiO<sub>2</sub>/perovskite interface. *Advanced Materials Interfaces* 2016; 3 (22). doi: 10.1002/admi.201600729
19. Noel NK, Abate A, Stranks SD, Parrott ES, Burlakov VM et al. Enhanced photoluminescence and solar cell performance via Lewis base passivation of organic-inorganic lead halide perovskites. *ACS Nano* 2014; 8 (10): 9815–9821. doi: 10.1021/nn5036476
20. Zhang F, Song J, Zhang L, Niu F, Hao Y et al. Film-through large perovskite grains formation: Via a combination of sequential thermal and solvent treatment. *Journal of Materials Chemistry A* 2016; 4 (22): 8554–8561. doi: 10.1039/c6ta03115c
21. Guo Q, Yuan F, Zhang B, Zhou S, Zhang J et al. Passivation of the grain boundaries of CH<sub>3</sub>NH<sub>3</sub>PbI<sub>3</sub> using carbon quantum dots for highly efficient perovskite solar cells with excellent environmental stability. *Nanoscale* 2019; 11 (1): 115–124. doi: 10.1039/c8nr08295b
22. Ma Y, Zhang H, Zhang Y, Hu R, Jiang M et al. Enhancing the performance of inverted perovskite solar cells via grain boundary passivation with carbon quantum dots. *ACS Applied Materials and Interfaces* 2019; 11 (3): 3044–3052. doi: 10.1021/acsami.8b18867
23. Xue Q, Liu M, Li Z, Yan L, Hu Z et al. Efficient and stable perovskite solar cells via dual functionalization of dopamine semiquinone radical with improved trap passivation capabilities. *Advanced Functional Materials* 2018; 28 (18): 14–16. doi: 10.1002/adfm.201707444